

## Effect of physical and chemical parameters on the $\beta$ -Tricalcium phosphate synthesized by the wet chemical method

Asmaa Massit<sup>1</sup>, Majda Fathi<sup>1</sup>, Ahmed El Yacoubi<sup>1</sup>, Abdelilah Kholtei<sup>2</sup> and Brahim Chafik El Idrissi<sup>1,\*</sup>

<sup>1</sup>Chemical Team Materials Surfaces Interfaces, Laboratory Materials and Energetics, Faculty of Sciences, University Ibn Tofail, kenitra, Po Box 133, Kénitra, Morocco

<sup>2</sup>Laboratory Chemistry\_Biology Applied to Environment, Faculty of Sciences, University Moulay Ismail, Po Box 11201, Zitoun Meknes, Morocco

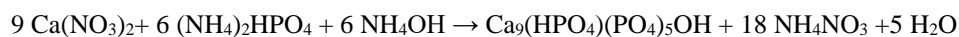
**Abstract:** In this paper, the synthesis of nanosized powders  $\beta$ -Tricalcium phosphate  $\beta$ -Ca<sub>3</sub>(PO<sub>4</sub>)<sub>2</sub> was studied by the wet chemical method at different values of reaction temperature, initial concentration of diammonium hydrogen phosphate (NH<sub>4</sub>)<sub>2</sub>HPO<sub>4</sub>, calcium nitrate tetrahydrate Ca(NO<sub>3</sub>)<sub>2</sub>·4H<sub>2</sub>O addition rate, pH of reaction and aging time. All these parameters have a great impact on the properties of the resulting  $\beta$ -TCP nano powders. Analysis results of morphology, structure of TCP powder from infrared (IR) spectra, X-ray diffraction (XRD) and transmission electron microscopy (TEM) indicated that the synthesized TCP powder had spherical crystal shape with crystallite size, calculated by XRD method, less than 60 nm, mono and biphasic structure composed of  $\beta$ -TCP with pyrophosphate calcium or hydroxyapatite. The variation of the synthesis conditions did not affect the morphology, but it affect the size of crystallites and particles.

**Keywords:**  $\beta$ -tricalcium phosphate; Wet chemical method; Synthesis conditions; crystallite size.

### Introduction

Tricalcium phosphate (TCP) is one of the variations of the calcium phosphate compounds with more applications in bone tissue regeneration<sup>1-3</sup>, due to its chemical composition Ca<sub>3</sub>(PO<sub>4</sub>)<sub>2</sub> being similar to the natural bone tissue<sup>4</sup>. TCP is widely used in the biomedical field because of excellent biocompatibility, high bioactivity, non-toxicity and non-inflammatory behaviour and non-immunogenic properties. It can exist in two possible forms,  $\alpha$  and  $\beta$ , and normally  $\beta$  form gets converted into  $\alpha$  with annealing at temperatures higher than 1250–1300°C<sup>5</sup>. The  $\beta$ -TCP is bioresorbable, and bioresorption occurs through osteoclastic activity<sup>6,7</sup>. It has good

biodegradability and higher dissolution rate in the body's environment after implantation, which is absorbed and replaced by new bone<sup>8</sup>. Many methods are used to synthesize of such biomaterials including wet-chemical method<sup>9,10</sup>, solid-state process<sup>11,12</sup> and microwave irradiation<sup>13,14</sup>, sol-gel, etc<sup>15,16</sup>. The most conventional is the precipitation in aqueous medium starting from Ca(NO<sub>3</sub>)<sub>2</sub> and (NH<sub>4</sub>)<sub>2</sub>HPO<sub>4</sub> as raw materials. It is noteworthy that  $\beta$ -TCP cannot be precipitated from solution, but only be prepared by calcination, e.g. of Apatitic tricalcium phosphate Ca<sub>9</sub>(HPO<sub>4</sub>)(PO<sub>4</sub>)<sub>5</sub>(OH) at temperatures over 750°C<sup>17</sup>.



However, the synthesis of a pure  $\beta$ -TCP by this method requires close control of many parameters such as reaction pH, temperature, the stoichiometry of the raw materials, ageing time. A slight variation of these experimental parameters can generate drastic variations in the composition of the final product<sup>18</sup>

and reveal the pyrophosphate calcium phase (Ca<sub>2</sub>P<sub>2</sub>O<sub>7</sub> or CPP) or the hydroxyapatite phase (Ca<sub>10</sub>(PO<sub>4</sub>)<sub>6</sub>(OH)<sub>2</sub> or HAp). These conditions remain specific and should be controlled by synthesis preparation parameters<sup>13,19</sup>. Therefore, it is crucial for biomedical applications to control some parameters of

\*Corresponding author: Brahim Chafik El Idrissi  
Email address: [chidrissi@yahoo.fr](mailto:chidrissi@yahoo.fr)  
DOI: <http://dx.doi.org/10.13171/mjc7310268-elidrissi>

Received August 12, 2018  
Accepted October 10, 2018  
Published October 26, 2018

TCP particles such as crystallite size, morphology and phase composition. Bioactivity of calcium phosphate materials depends on many factors during the synthesis procedure including precursor reagents, impurity contents, crystal size and morphology, concentration and mixture order of reagents, pH and temperature. Such conditions are application specific and should be controlled by synthesis preparation parameters<sup>13,19</sup>. Therefore, controlling crystallite size, morphology and phase composition of TCP is very important for biomedical applications.

In this paper, we present some results of  $\beta$ -TCP nanopowder synthesized by the wet chemical method and the effects of synthetic conditions, i.e. reaction temperature, ageing time, pH of mixture solution,  $(\text{NH}_4)_2\text{HPO}_4$  addition rate and reactant concentration on crystallite size, fraction of crystallinity and morphology.

### Materials and Methods

Tricalcium phosphate was synthesized by the wet chemical method using  $(\text{NH}_4)_2\text{HPO}_4$  solution at the various  $(\text{NH}_4)_2\text{HPO}_4$  (Riedel-de Haën, Germany) concentrations 0.15, 0.20, 0.25M in distilled water. The  $\text{Ca}(\text{NO}_3)_2 \cdot 4\text{H}_2\text{O}$  (Scharlau, Spain) concentration was set at 0.36M to obtain the Ca/P molar ratio of 1.50. Its solution was added dropwise into  $(\text{NH}_4)_2\text{HPO}_4$  solution with addition rate of 3, 30 and 300 ml min<sup>-1</sup> under a constant stirring condition. During the synthesizing process, the pH value varies between 7 and 9. The pH of the solution was adjusted by the addition of ammonium hydroxide  $\text{NH}_4\text{OH}$ . The reaction was conducted at different temperatures (30, 40, 50, 60 and 70°C). This precipitated solution was stirred for 2 h and aged at room temperature (RT) for different times (2, 24, 48 and 72h). The precipitate was filtered and washed repeatedly using distilled water to remove  $\text{NH}_4^+$  and  $\text{NO}_3^-$  ions. The resultant precipitate was dried at 70°C for 24 h in a dry oven

and then crushed in a mortar. The powders were calcined at 800°C for 1 h.

The phase purity and crystallinity of the TCP powder were analyzed by X-ray diffraction (XRD) (XPRT-PROPW3050/60 ( $\theta/\theta$ ) using  $\text{CuK}\alpha$  radiation  $\lambda = 1.54056 \text{ \AA}$  and operating at 45 kV and 40 mA, step angle of 0.03° and  $2\theta$  in range of 15–60°. Crystalline phases detected in the patterns were identified by comparison to the standard patterns from the ICDD-PDF (International Center for Diffraction Data-Powder Diffraction Files). The crystallite dimensions (D) were calculated using Debye-Scherrer Eq. (1):

$$D = 0.9 \lambda / \text{FWHM} \cdot \cos\theta \quad (1)$$

Where D is the crystallite size (nm),  $\lambda$  the wavelength of X-ray beam (0.15406 nm for  $\text{Cu-K}\alpha$  radiation), FWHM the full width at half maximum for the diffraction peak under consideration (rad), and  $\theta$  is the diffraction angle (°). The crystallinity noted by Xc corresponds to the fraction of crystalline  $\beta$ -TCP phase in the investigated volume of powdered sample, evaluated by the Eq (2):

$$\text{Xc} = 1 - V_{300/0210}/I_{0210} \quad (2)$$

Where  $I_{0210}$  is the intensity of (0 2 10) reflection of  $\beta$ -TCP structure and  $V_{300/0210}$  is the intensity of the hollow between (3 0 0) and (0 2 10) reflections<sup>20,21</sup>.

The characteristic functional groups of  $\beta$ -TCP were identified by Fourier transform infrared (FTIR) spectroscopy, VERTEX 70, Genesis Series (400–4000 cm<sup>-1</sup>, resolution 4, scans 20). For this 1% of the powder was mixed and ground with 99% KBr and the spectrum was taken in the range of 400 to 4000 cm<sup>-1</sup>.

The size and morphology of fine TCP powder were observed on a transmission electron microscope (Philips CM10, Eindhoven, The Netherlands) that operated at the acceleration voltage of 100 kV.

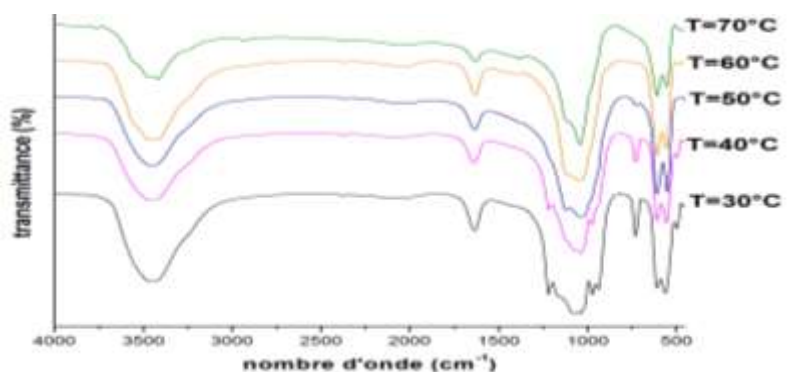


**Figure 1.** IR spectra of TCP powder synthesized at different temperatures.

### Results and Discussion

The reaction temperature was an important factor that could affect the morphology, the phase structure

and the crystallinity of the synthesized TCP powder. (Fig. 1) and Table 1 show the FTIR spectra and the bonds of the functional groups of the TCP powder synthesized using  $\text{Ca}(\text{NO}_3)_2 \cdot 4\text{H}_2\text{O}$  and  $(\text{NH}_4)_2\text{HPO}_4$

solution at the different reaction temperatures, with  $(\text{NH}_4)_2\text{HPO}_4$  concentration of 0.15M and at an addition rate of about 300 ml/min, at an aging time of 2 h and at a pH of about 9. The IR spectra of all synthesized samples showed the characteristic peaks corresponding to  $\beta$ -TCP<sup>22</sup>. The bands at 1043 and 1078  $\text{cm}^{-1}$  corresponded to the triple degenerate  $\nu_3$  antisymmetric stretching vibration of  $\text{PO}_4^{3-}$ . 968  $\text{cm}^{-1}$  band was assigned to  $\nu_1$ , the symmetric stretching vibration of  $\text{PO}_4^{3-}$ . The bands at 607 and 559  $\text{cm}^{-1}$

corresponded to the triple degenerate  $\nu_4$  antisymmetric stretching mode. The peak and the broad band of the single molecule of adsorbed water were also discerned at 1633 and between 3700 and 3100  $\text{cm}^{-1}$  respectively. Moreover, the FTIR had shown the presence, at 729 and 1218  $\text{cm}^{-1}$ , of  $\text{P}_2\text{O}_7^{4-}$  group, which is characteristic to the calcium pyrophosphate phase  $\beta\text{-Ca}_2\text{P}_2\text{O}_7$  (JCPDF 9-346). With the temperature rising, these bands become narrower and low then gradually disappear.

**Table 1.** Wave numbers for the functional groups of TCP.

Functional groups	$\nu_1$ ( $\text{PO}_4^{3-}$ )	$\nu_2$ ( $\text{PO}_4^{3-}$ )	$\nu_3$ ( $\text{PO}_4^{3-}$ )	$\nu$ (HOH)	$\nu$ ( $\text{P}_2\text{O}_7^{4-}$ )
$\nu(\text{cm}^{-1})$	968	559 607	1043 1078	1633 3450	729 1218

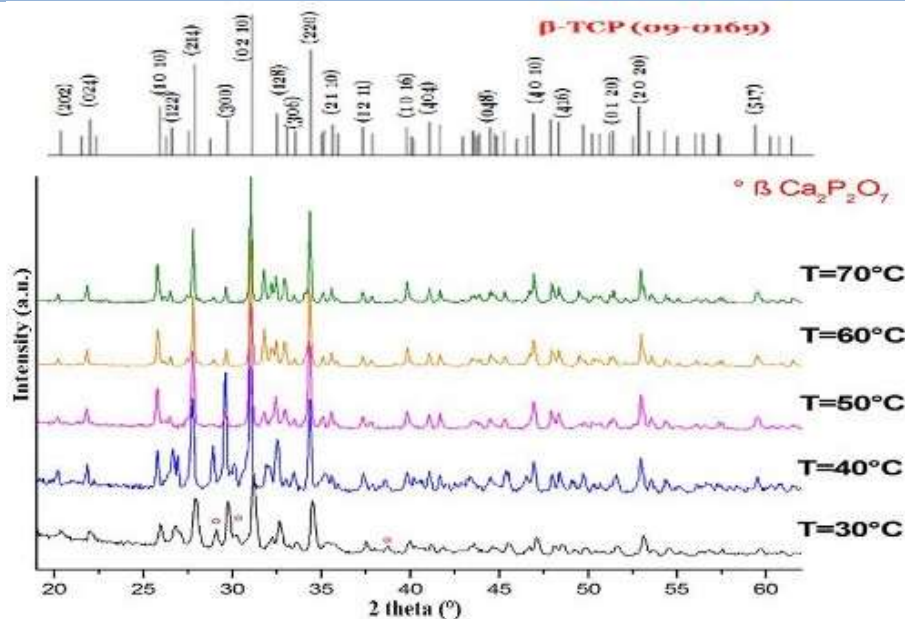


**Figure 2.** XRD spectra of TCP powder synthesized at different temperatures.

The XRD spectra of the TCP powder synthesized at the various temperatures are shown in (Fig. 2). All XRD patterns show diffraction peaks characteristics of  $\beta$ -Tricalcium phosphate presents in standards and in literature. The major phase, as expected, is  $\beta$ -TCP, which is confirmed by comparing data obtained with the ICDD PDF 009-0169. Powders exhibited sharp

diffraction peaks indicating high crystallinity. Conversely, in the  $\beta$ -TCP powders prepared at reaction temperatures 30 and 40°C, and in agreement with the previous FTIR results, besides the  $\beta$ -TCP, an additional peak is detected at  $2\theta = 28.9^\circ$  such peak corresponds to  $\beta$ -CPP phase.

**Table 2.** The crystal diameter and crystallinity of TCP powder synthesized at different temperatures.

Temperature (°C)	Crystal Diameter (nm)	Crystallinity $X_c$
30	20	93
40	37	97
50	41	99
60	55	99
70	59	99

The TCP crystal diameter calculated from the Scherrer equation showed that the crystal diameter and degree of crystallinity increased from 20 to 59 nm and from 93 to 99 on increasing the reaction temperature from 30 to 70°C, respectively Table 2.

Increasing the temperature results in faster motion of molecules, so there was an increased chance of therm colliding with each other; the TCP particles concentrated to form larger particles. At 30°C, the TCP particle had the smallest diameter. It has been

found that the control of the crystallinity of calcium phosphates is necessary for their biological applications<sup>23</sup>. Since calcium phosphates with low-level of crystallinity show high osteoconductivity, the synthesized powders can be used to promote osseointegration or used as a coating to promote bone in growth into prosthetic implants<sup>24</sup>.

#### Effect of reactant concentration

By varying the precursor concentration, the kinetics of TCP precursor synthesis can be affected. By increasing the precursor concentration, the solubility limit at a given pH is more rapidly exceeded, creating a burst of primary nuclei for crystal growth. However, as the reactants are

continually added, the primary nuclei continue to grow rapidly high precursor concentrations resulted in larger crystallite and particle sizes. (Fig. 3) presents the IR spectra of the TCP powder obtained at various initial concentrations of  $(\text{NH}_4)_2\text{HPO}_4$  solution at room temperature, at an addition rate of about 300 ml/min, at an ageing time of 48 h and at a pH of about 9. It could be found that the IR spectra of the TCP samples had the same shapes and the characteristic peaks of the functional groups of TCP are shown. The very weak band of the secondary phase,  $\text{P}_2\text{O}_7$  at  $728\text{ cm}^{-1}$ , gradually disappeared during the decrease in the concentration of  $(\text{NH}_4)_2\text{HPO}_4$  solution from 0.25 to 0.15.

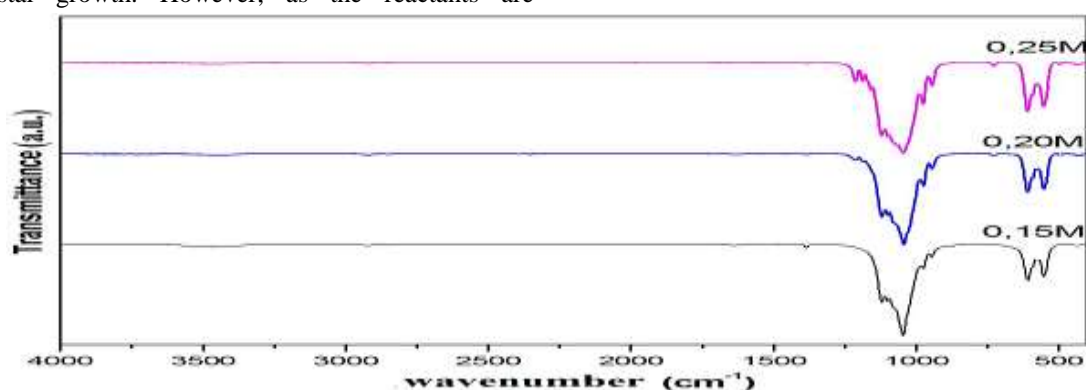


Figure 3. IR spectra of the TCP samples synthesized at different initial concentrations of  $(\text{NH}_4)_2\text{HPO}_4$  solution

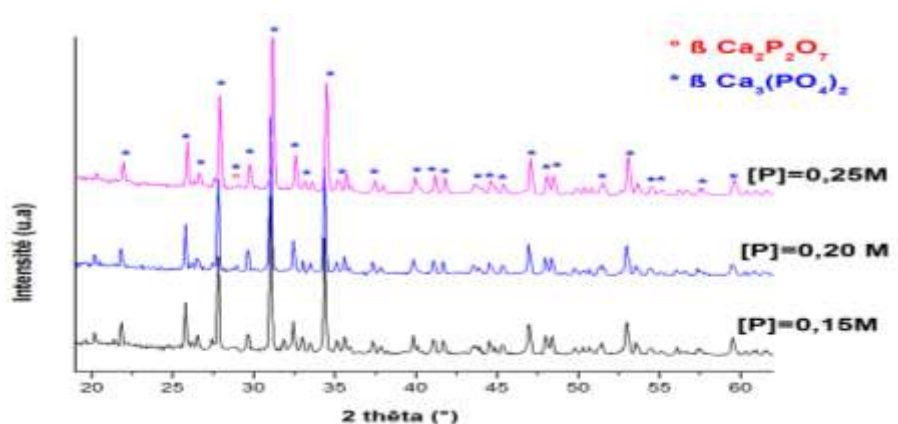


Figure 4. IR spectra of the TCP samples synthesized at different initial concentrations of  $(\text{NH}_4)_2\text{HPO}_4$  solution

(Fig. 4) and Table 3 introduce XRD spectra and XRD-calculated crystal diameters and crystallinity, respectively. In general, XRD patterns of the TCP samples had the same shapes and had only the characteristic peaks of the TCP molecule. The insignificant amount of  $\text{Ca}_2\text{P}_2\text{O}_7$  detected by FTIR in the samples synthesized with 0.25 and 0.2M is

undetectable by XRD. For powder prepared at 0.15 M, besides the  $\beta$ -TCP, an additional small peak is detected at  $2\theta = 31.8^\circ$  such peak corresponds to Hap (JCPDS 9-0432) phase. The crystal diameter was in a range from 40 to 51 nm. XRD analysis also shows a weak effect of reacting concentration (in the above-mentioned range) on the TCP crystal diameter.

Table 3. The crystal diameter and crystallinity of TCP powder synthesized at various  $(\text{NH}_4)_2\text{HPO}_4$  concentrations.

Concentration of $(\text{NH}_4)_2\text{HPO}_4$ (M)	Crystal Diameter (nm)	Crystallinity $X_c$
0.15	48	99
0.20	51	99
0.25	40	99

### Effect of $\text{Ca}(\text{NO}_3)_2$ addition rate

The adding rate of  $\text{Ca}(\text{NO}_3)_2$  affects the morphology, structure and size of formed TCP crystals. By varying the precursor addition rate, nucleation and crystal growth rates can be controlled. Rapid addition of precursors results in localized high concentrations of precursors, exceeding the solubility of TCP in those regions, which favors nucleation and

formation of small crystals<sup>25</sup>. (Fig. 4) presents the IR spectra of the samples synthesized with the dropping rates of 3, 30 and 300  $\text{ml}\cdot\text{min}^{-1}$  at RT, at an ageing time of 48 h and at a pH of about 9. All IR spectra of the samples have similar shapes and the specific peaks corresponding to functional groups in the  $\beta$ -TCP molecule. The bands at 725 and 1200  $\text{cm}^{-1}$  indicated the presence of  $\text{P}_2\text{O}_7^{4-}$  groups.

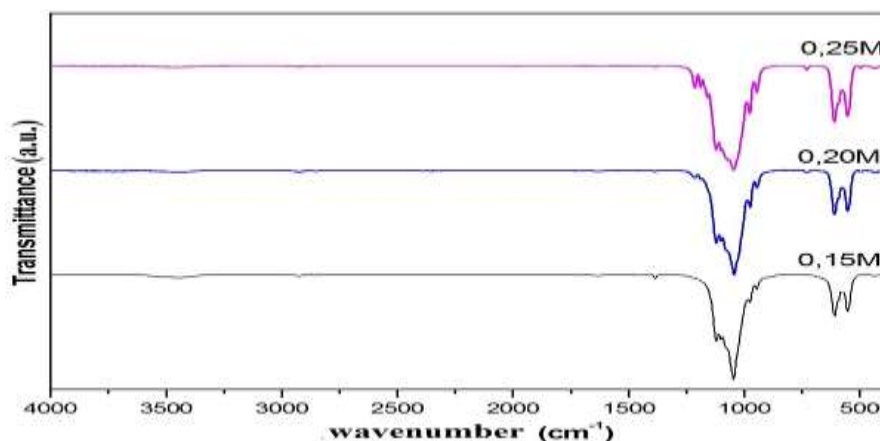


Figure 5. IR spectra of TCP powder synthesized at different  $\text{Ca}(\text{NO}_3)_2$  addition's rates

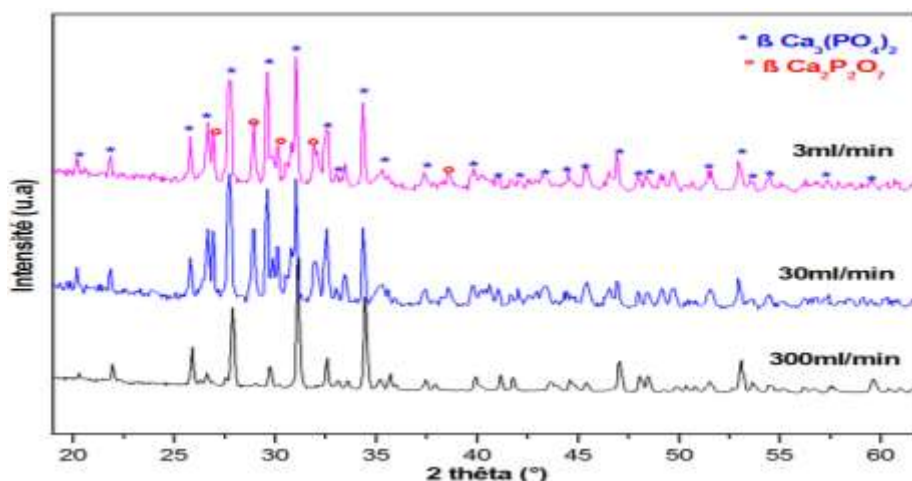


Figure 6. X-ray spectra of TCP powder synthesized at different  $\text{Ca}(\text{NO}_3)_2$  addition's rates

(Fig. 6) and Table 4 introduce XRD spectra and XRD-calculated crystal diameters and crystallinity, respectively. XRD patterns of the  $\beta$ -TCP samples had the same shapes and had all the characteristics peaks of the molecule. The diffractograms of the samples

prepared with a precursor addition rate of 30  $\text{ml}/\text{min}$  and 3  $\text{ml}/\text{min}$  show additional peaks relative to the group  $\text{P}_2\text{O}_7$ . From this table, it was found that when  $\text{Ca}(\text{NO}_3)_2$  adding rate increased the crystal diameter decreases and crystallinity increases.

Table 4. The crystal diameter, crystallinity and average particle size of TCP powder synthesized at different  $\text{Ca}(\text{NO}_3)_2\cdot 4\text{H}_2\text{O}$  addition rates.

$\text{Ca}(\text{NO}_3)_2$ addition Rate (ml/min)	Crystal Diameter (nm)	Crystallinity $X_c$	Average particle Size (nm)
3	56	72	-
30	54	75	130-300
300	40	94	80-200

To confirm the XRD results, the morphology of TCP powder was further analyzed by TEM images. (Fig. 7) and Table 4 present the TEM images and TEM-based calculated average particle sizes. TCP

particle had a spherical shape and highly agglomerated. It has been found that nanoparticles with spherical morphology are better than other irregular morphologies due to the good space fillings

and the low percentage of voids in the final product<sup>26</sup>. However, when  $\text{Ca}(\text{NO}_3)_2$  adding rate increased, particle size decreased. These results allowed

concluding that the slow addition of precursors results in a regime favouring crystal growth and formation of larger particles.

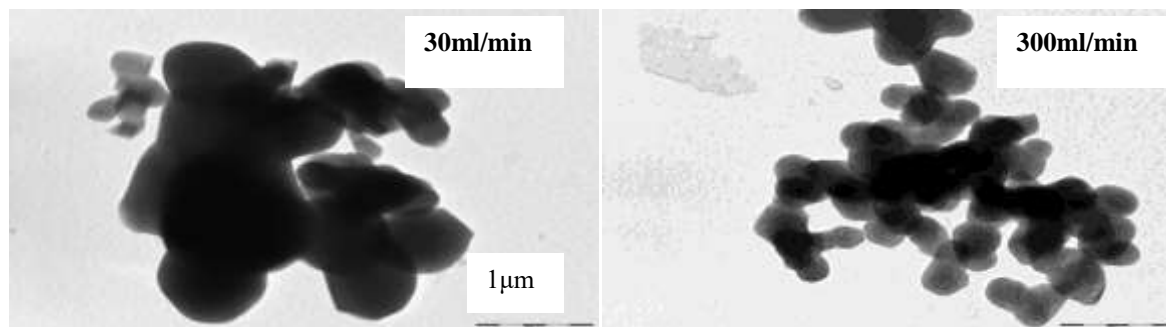


**Figure 7.** TEM images of TCP samples synthesized at a various addition rate

### Effect of pH of the reaction

Two parameters govern which phase will form for a given calcium phosphate: the initial calcium to phosphate ratio of the reactants and the pH at which the reaction occurs. We synthesized TCP powder by dropping slowly  $\text{Ca}(\text{NO}_3)_2 \cdot 4\text{H}_2\text{O}$  solution into  $(\text{NH}_4)_2\text{HPO}_4$  solution at room temperature with various pH 7, 8 and 9 at an ageing time of 24 h. The IR spectra of TCP powder synthesized at three pH values are shown in (Fig. 8). By comparing these IR

results with data in Table 1, it was found that the obtained TCP had all the characteristic peaks of TCP. The very weak bands of the secondary phase,  $\text{Ca}_2\text{P}_2\text{O}_7$  at 727 and 1213  $\text{cm}^{-1}$  appear in the sample synthesized with pH=7. Also, the XRD results indicated the characteristic diffraction peaks of TCP, and no other phases of calcium phosphate were detected (Fig. 9) except for the spectrum of the sample synthesized with pH=7 shows additional peak characteristic of the  $\beta\text{-Ca}_2\text{P}_2\text{O}_7$  phase.

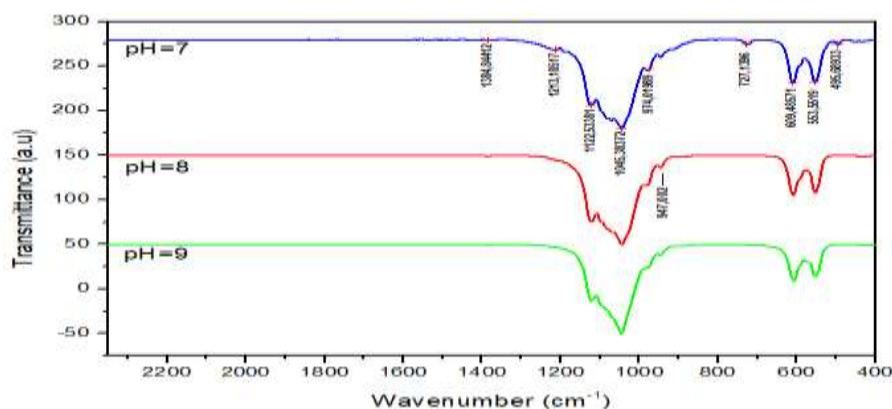


**Figure 8.** IR spectra of TCP powder synthesized at different pH values

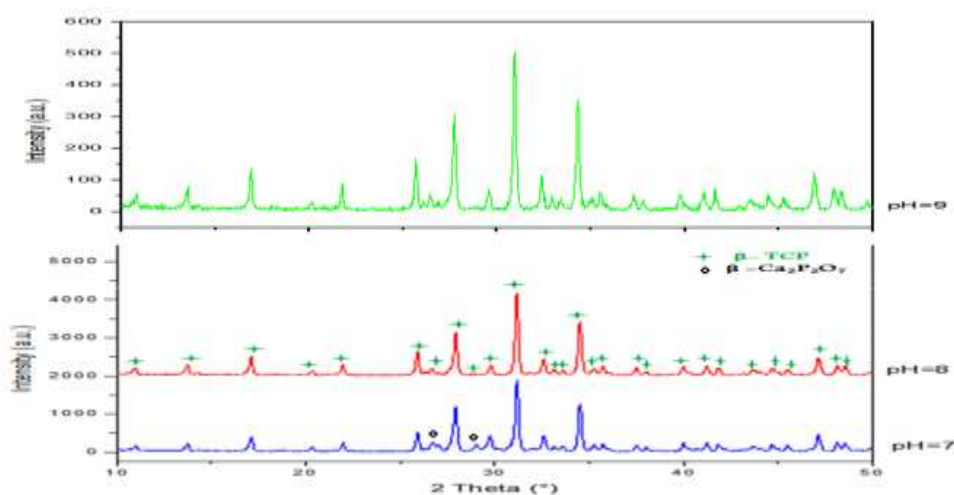


**Figure 9.** X-ray spectra of TCP powder synthesized at different pH values

The data in Table 5 shows that the degree of crystallinity increase and become stable at pH = 8, XRD analyses also demonstrate a weak effect of pH (in the above-mentioned range) on the TCP crystal

diameter, when the pH increased from 7 to 9 the crystallite size did not increase significantly, only from 40 to 43 nm.

**Table 5.** The crystal diameter, crystallinity and average particle size of TCP powder synthesized at different pH values.

pH values of The reaction	Crystal Diameter (nm)	Crystallinity $X_C$	Average particle Size (nm)
7	40	77	150-180
8	41	86	150-180
9	43	86	150-180

(Fig. 10) and Table 5 show the TEM images and average particle size of TCP calculated from the TEM images, respectively. The pH did not affect the morphology of TCP powder. As for the TEM results, it could be found that the TCP crystals had a spherical shape.

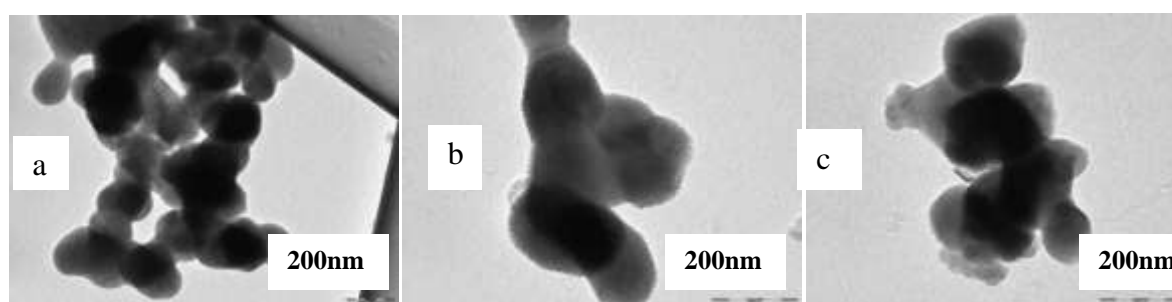


**Figure 10.** TEM images of TCP samples synthesized at pH=7 (a), pH=8 (b) and pH=9 (c)

#### Effect of ageing time

The crystallinity and structural development of TCP is also affected by varying the ageing time of the precipitate. Longer ageing times ensure that reagents are fully reacted and precipitate out of the solution. The IR spectra of TCP samples prepared at 25°C, pH = 9 with various ageing times 2, 24, 48 and 72 hours are shown in (Fig. 11). By comparing these IR results with data in Table 1, it was found that the spectrums are similar to that of  $\beta$ -TCP, also, at 727, 1190 and 1213  $\text{cm}^{-1}$ , we can observe the presence of  $\text{P}_2\text{O}_7^{4-}$  group.

The XRD spectra of TCP powder prepared at different ageing times are represented in (Fig. 12). The characteristic diffraction peaks of TCP are indicated. The results showed that TCP synthesized at the different ageing time had the main crystalline phase present. The powder 72h presents a slight shift in XRD peaks towards lower theta value; this may be due to the elongation in the crystal structure. Also, a minor amount of pyrophosphate was also found. However, the crystallite size and the degree of crystallinity increase with ageing time and become stable after 48h for both (Table 6)

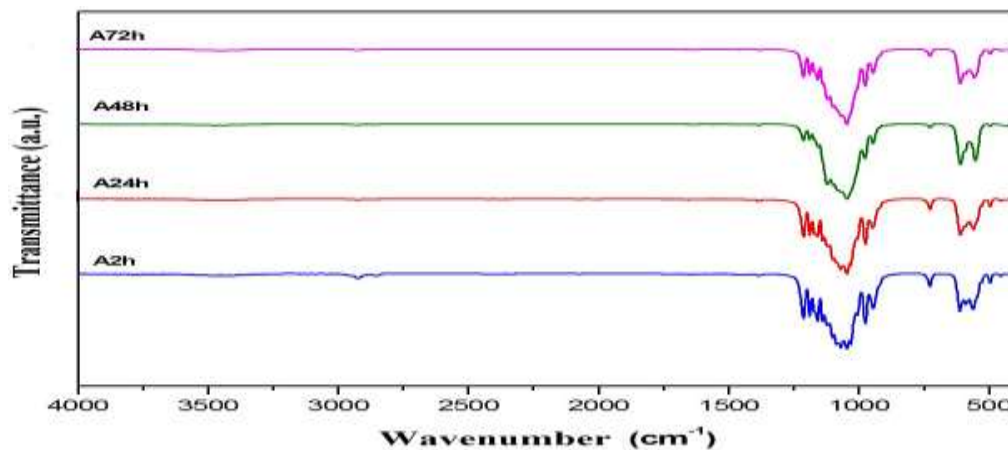


**Figure 11.** IR spectra of TCP powder synthesized at different ageing times

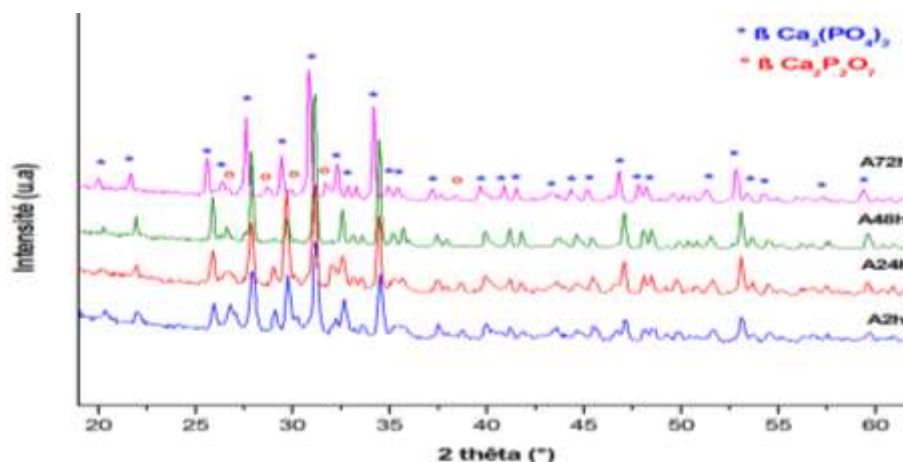


**Figure 12.** X-ray spectra of TCP prepared at different ageing times

The TEM images of TCP powder prepared at ageing times 2h and 72 h are presented in (Fig. 13), At different ageing times, all obtained TCP had

almost spherical and strongly agglomerated particles. The data in Table 6 shows that the particle size slightly increased with increasing ageing time.

**Table 6.** The crystal diameter, crystallinity and average particle size of TCP powder synthesized at the different ageing time.

Ageing time (hours)	Crystal Diameter (nm)	Crystallinity $X_C$	Average particle Size (nm)
2	32	83	~300
24	42	86	-
48	42	95	-
72	42	94	~400

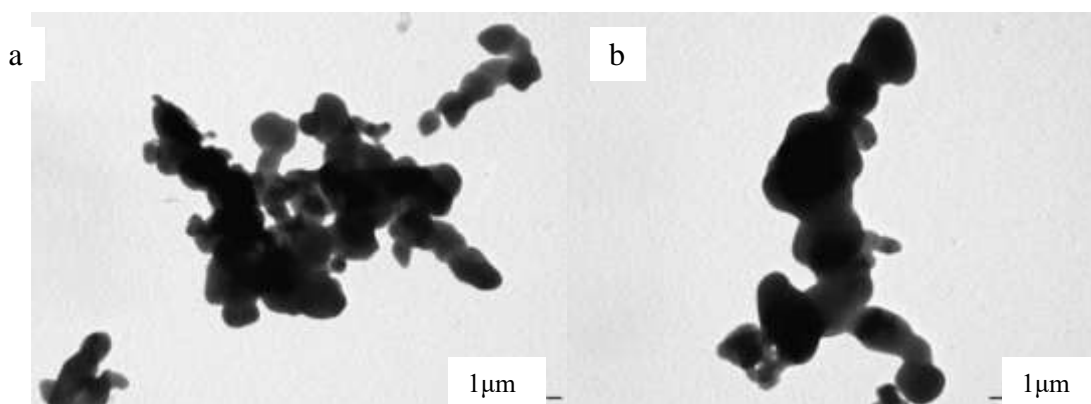


**Figure 13.** TEM images of TCP samples synthesized at different ageing times: (a) 2h, (b) 72h

## Conclusion

Nano-sized  $\beta$ -Tricalcium phosphate powder was synthesized by the wet chemical method, by varying process parameter, followed by calcination, using calcium nitrate, diammonium phosphate solution as reactants, and ammonia as adjusting agent. The obtained results showed that the synthetic conditions were important in controlling the quality, shape and size of the TCP powder, but had significant effects on morphology. The calcined powders show the presence of two distinguishable crystalline phases  $\beta$ -Tricalcium phosphate and  $\beta$ -pyrophosphate or hydroxyapatite, spherical shape, crystallite size less than 60nm and a high degree of crystallinity. All the results obtained allow determining the optimal

conditions for synthesizing pure nanosized  $\beta$ -TCP with a high degree of crystallinity and a crystalline size of less than 50 nm. Indeed, a synthesis temperature of 50 °C, a dropping rate of 300ml.min<sup>-1</sup>, ageing time of 48h and a pH of about 9 are considered as the best synthesis conditions.

## References

- 1- A. Tevlek, P. Hosseinian, C. Ogutcu, M. Turk, H.M. Aydin, Bi-layered constructs of poly (glycerol-sebacate) tricalcium phosphate for bone-soft tissue interface applications, Mater. Sci. Eng. C, **2017**, 72, 316–324.
- 2- S. Hoover, S. Tarafder, A. Bandyopadhyay, S. Bose, Silver doped resorbable tricalcium phosphate scaffolds for bone graft applications,

- Mater. Sci. Eng. C, **2017**, 79, 763–769.
- 3- J. Park, S.J. Lee, H.H. Jo, J.H. Lee, W.D. Kim, J.Y. Lee, S.A. Park, Fabrication and characterization of 3D-printed bone-like -tricalcium phosphate/polycaprolactone scaffolds for dental tissue engineering, *J. Ind. Eng. Chem.*, **2017**, 46, 175–181.
- 4- B.T. Smith, M. Santoro, E.C. Grosfeld, S.R. Shah, J.J.J.P. van den Beucken, J.A. Jansen, A.G. Mikos, Incorporation of fast dissolving glucose porogens into an injectable calcium phosphate cement for bone tissue engineering, *Acta Biomater.*, **2017**, 50, 68–77.
- 5- M. Fathi, A. El Yacoubi, A. Massit, B. Chafik El Idrissi, Wet chemical method for preparing high purity  $\beta$  and  $\alpha$ - tricalcium phosphate crystalline powders, *IJSER*, vol6, Iss6, **2015**, 139-143.
6. Cen Y, Zhang TH, Gan CH, Yu G Wear studies of hydroxyapatite composite coating reinforced by carbon nanotubes. *Carbon*, **2007**, 45, 998-1004.
7. Klein CPAT, Driessen AA, Groot K, Hoof A Biodegradation behavior of various calcium phosphate materials in bone tissue. *J Biomed Mater Res*, **1983**, 17, 769-784.
- 8- L. Sha, Y. Liu, Q. Zhang, M. Hu, and Y. Jiang, Microwave-assisted co-precipitation synthesis of high purity  $\beta$ -tricalcium phosphate crystalline powders, *Materials Chemistry and Physics*, vol. 129, no. 3, **2011**, 1138–1141.
- 9- Y. Pan, J.L. Huang, C.Y. Shao, Preparation of  $\beta$ -TCP with high thermal stability by solid reaction route, *J. Mater.Sci.*, **2003**, 38, 1049–1056.
- 10- B. Chafik El Idrissi, K. Yamni, A. Yacoubi, A. Massit, A novel method to synthesize nanocrystalline hydroxyapatite: Characterization with x-ray diffraction and infrared spectroscopy, *IOSR Journal of Applied Chemistry* Vol7, Issue 5 Ver. III, **2014**, 107-112.
- 11- S.C. Liou, S.Y. Chen, Transformation mechanism of different chemically precipitated apatitic precursors into  $\beta$ -tricalcium phosphate upon calcination, *Biomaterials*, **2002**, 23, 4541–4547.
- 12- A. Cuneyt Tas, F. Korkusuz, M. Timucin, N. Akkas, An Investigation of the Chemical Synthesis and High-Temperature Sintering Behaviour of Calcium Hydroxyapatite (HA) and Tricalcium Phosphate (TCP) *Bioceramics*, *J. Mater.Sci.Mater.Med.*, **1997**, 8, 91–96.
- 13- A. Farzadi, M. Solati-Hashjin, F. Bakhshi, A. Aminian, Synthesis and characterization of hydroxyapatite/b-tricalcium phosphate nanocomposites using microwave irradiation, *Ceramics International*, **2011**, 37, 65–71.
- 14- Li Shaa, YuyanLiub, Qing Zhanga, Min Hub, Yinshan Jiang, Microwave-assisted co-precipitation synthesis of high purity tricalcium phosphate crystalline powders, *Materials Chem and Phys*, **2011**, 129, 1138–1141.
- 15- M.B. Thürmer, C.E. Diehl, L.A.L. dos Santos, Calcium phosphate cements based on alpha-tricalcium phosphate obtained by wet method: synthesis and milling effects, *Ceram. Int.*, **2016**, 42, 18094–18099.
- 16- C. Ruiz-Aguilar, et al., Characterization of -tricalcium phosphate powders synthesized by sol-gel and mechanosynthesis, *Bol. Soc. Esp. Cerám. Vidr.* **2018**, 213-220.
- 17- A. Destainville, E. Champion, D. Bernache-Assollant, E. Laborde, Synthesis, characterization and thermal behaviour of apatitic tricalcium phosphate, *Materials Chemistry and Physics*, **2003**, 80, 269–277.
- 18- S. Raynaud, E. Champion, D. Bernache-Assollant, J.-P. Laval, Determination of calcium/phosphate atomic ratio of calcium phosphate apatites using X-ray diffractometry, *J.Am. Ceram. Soc.*, **2001**, 84, 359-366.
- 19- M. Santos, M. Oliveira, L. Souza, H. Mansur, W. Vasconcelos, Synthesis Control and Characterization of Hydroxyapatite Prepared by Wet Precipitation Process, *Materials Research*, **2004**, 7, 625–630.
- 20- R.G. Carrodeguas, A.H. De Aza, I. Garcia-Paez, S. De Aza, P. Pena, Revisiting the Phase-Equilibrium Diagram of the  $\text{Ca}_3(\text{PO}_4)_2$ - $\text{CaMg}(\text{SiO}_3)_2$  System, *J. Am. Ceram. Soc.*, **2010**, 93, 561–569.
- 21- K.P.Sanosh, Min-Cheol Chu, A.Balakrishnan, T.N.Kim, Seong-JaiCho, Sol-gel synthesis of pure nano-sized  $\beta$ -tricalcium phosphate crystalline powders, *Current Applied Physics*, **2010**, 10, 68-71.
- 22- B. Nasiri-Tabrizi, A. Fahami, Production of poorly crystalline tricalcium phosphate nanopowders using different mechanochemical reactions, *J. Ind. Eng. Chem.* **2014**, 1236-1242.
- 23- T. Nakano, A. Tokumura, Y. Umakoshi, Variation in crystallinity of hydroxyapatite and the related calcium phosphates by mechanical grinding and subsequent heat treatment, *Metallurgical and Materials Transactions A*, **2002**, 33, 521-528.
- 24- K.P. Sanosh, M.C. Chu, A. Balakrishnan, Y.J. Lee, T.N. Kim, S.J. Cho, Synthesis of nano-hydroxyapatite powder that simulates teeth particle morphology and composition, *Current Applied Physics*, **2009**, 9, 1459-1462.
- 25- A. Massit, A. El Yacoubi, A. Rezzouk, B. Chafik El Idrissi, Preparation of Tricalcium phosphate: effect of precursor addition rate on the microstructural properties, *IJASTR*, Issue 5 vol 4, **2015**, 617-625.
- 26- B. Nasiri-Tabrizi, A. Fahami, R.Ebrahimi-Kahrizangi, Effect of milling parameters on the formation of nanocrystalline hydroxyapatite using different raw materials in, *Ceramics International*, **2013**, 39, 5751-5763.